



Robotic-assisted CT-guided percutaneous pulmonary nodules localization by hook-wire needles: a retrospective observational study

Haoming Guo, Zubin Ouyang, Xinghua Li, Yongliang Han, Fengming Tao, Mengqi Liu, Runtian Cheng, Xiaoya Chen, Fajin Lv, Haitao Yang

Department of Radiology, the First Affiliated Hospital of Chongqing Medical University, Chongqing, China

Contributions: (I) Conception and design: H Yang; (II) Administrative support: F Lv; (III) Provision of study materials or patients: Z Ouyang, X Li, Y Han, F Tao, M Liu, R Cheng, X Chen; (IV) Collection and assembly of data: H Guo, Z Ouyang, X Li; (V) Data analysis and interpretation: H Guo, H Yang; (VI) Manuscript writing: All authors; (VII) Final approval of manuscript: All authors.

Correspondence to: Haitao Yang, MD, PhD. Department of Radiology, the First Affiliated Hospital of Chongqing Medical University, 1 Youyi Road, Yuzhong District, Chongqing 400016, China. Email: frankyang119@126.com.

Background: Preoperative computed tomography (CT)-guided localization of small pulmonary nodules (SPNs) is the major approach for accurate intraoperative visualization in video-assisted thoracoscopic surgery (VATS). However, this interventional procedure has certain risks and may challenge to less experienced junior doctors. This study aims to evaluate the feasibility and efficacy of robotic-assisted CT-guided preoperative pulmonary nodules localization with the modified hook-wire needles before VATS.

Methods: A total of 599 patients with 654 SPNs who preoperatively accepted robotic-assisted CT-guided percutaneous pulmonary localization were respectively enrolled and compared to 90 patients with 94 SPNs who underwent the conventional CT-guided manual localization. The clinical and imaging data including patients' basic information, pulmonary nodule features, location procedure findings, and operation time were analyzed.

Results: The localization success rate was 96.64% (632/654). The mean time required for marking was 22.85 ± 10.27 min. Anchor of dislodgement occurred in 2 cases (0.31%). Localization-related complications included pneumothorax in 163 cases (27.21%), parenchymal hemorrhage in 222 cases (33.94%), pleural reaction in 3 cases (0.50%), and intercostal vascular hemorrhage in 5 cases (0.83%). Localization and VATS were performed within 24 hours. All devices were successfully retrieved in VATS. Histopathological examination revealed 166 (25.38%) benign nodules and 488 (74.62%) malignant nodules. For patients who received localizations, VATS spent a significantly shorter time, especially the segmentectomy group (93.61 ± 35.72 vs. 167.50 ± 40.70 min, $P < 0.001$). The proportion of pneumothorax in the robotic-assisted group significantly decreased compared with the conventional manual group (27.21% vs. 43.33%, $P = 0.002$).

Conclusions: Robotic-assisted CT-guided percutaneous pulmonary nodules hook-wire localization could be effectively helpful for junior less experienced interventional physicians to master the procedure and potentially increase precision.

Keywords: Robotic-assisted; pulmonary nodules; computed tomography-guided localization (CT-guided localization); robotic navigation

Submitted Feb 02, 2024. Accepted for publication May 17, 2024. Published online Jul 04, 2024.

doi: 10.21037/jtd-24-198

View this article at: <https://dx.doi.org/10.21037/jtd-24-198>

Introduction

Following the wide application of low-dose computed tomography (CT) for lung cancer screening, it has improved survival and reduced mortality of lung cancer by detecting and treating the early stage of lung cancer that often presents as the small pulmonary nodules (SPNs) (1). Wedge lung resection and segmentectomy have become more accepted and popular, especially in patients with SPNs suspected to be malignant, due to with similar tumor prognosis to lobectomy but better postoperative respiratory function and quality of life (2). The accurate intraoperative detection of the small and ground-glass nodules (GGNs) observed on CT is very important for wedge or segmental lung resection. However, these nodules are frequently difficult to identify during surgery, particularly in performing minimally invasive video-assisted thoracoscopic surgery (VATS), due to their small size, deep location, soft density, and limited operative channel. Nearly half of GGNs were missed or failed to be visualized or palpated during unguided VATS excision (2-4).

With the high demand of preoperative localization and intraoperative visualization of the SPNs, preoperative CT-guided localization has proved to be the major approach that renders GGN 'visible' (3-6). However, the accuracy of CT-guided manipulation is highly dependent on the operator's experience, which easily injures surrounding vulnerable structures like vessels and nerves if there are needle placement errors. Conventional freehand localization

requires multiple punctures, adjustments, and verifications, especially by less experienced junior interventional physicians. A new robotic-assisted navigational system has been reported to offer a tailored solution to simplify the technically challenging procedure and reduce the radiation dose and complication rate, especially useful for less skilled interventional physicians (7-9). Several marker materials with needle-mediated techniques have also been utilized in preoperative localization including the placement of a hook wire, microcoil, lipiodol, and injection of methylene blue and a radioactive isotope (10). Recently a modified hook-wire needle tailored for SPNs has been reported as safe, with a high success rate, feasibility, and good tolerance (11-15).

To date, robot-assisted localization of pulmonary nodules has not been evaluated. This study aimed to combine the modified localization device with the robotic navigated CT guidance in targeting preoperative SPNs. We shared our experience to report our techniques, localization success rate, operative complications, and lessons learned over time. We present this article in accordance with the STROBE reporting checklist (available at <https://jtd.amegroups.com/article/view/10.21037/jtd-24-198/rc>).

Methods

Patients

This retrospective study was approved by the Ethics Committee for Human Research of the First Affiliated Hospital of Chongqing Medical University (No. ES-2023-020-01). A total of 599 consecutive patients who underwent preoperative CT-guided localization of SPNs between 1 December 2020 and 31 December 2021 in the First Affiliated Hospital of Chongqing Medical University were retrospectively enrolled in this study and the electronic chart records were reviewed with CT images on the Picture Archiving and Communication System (PACS). The requirement for informed consent was waived for this retrospective analysis. The study was conducted in accordance with the Declaration of Helsinki (as revised in 2013). Inclusion criteria were solitary or multiple SPNs suspected as having malignant possibility and performed VATS on the same day in our hospital. Exclusion criteria were as follows: (I) SPNs diameter >30 mm; (II) patient with obvious emphysema, pulmonary hypertension, pulmonary fibrosis, and other cardiopulmonary disease; (III) existing massive bullae or vessels in the puncture route; and (IV) patient with coagulation disorders or severe infection.

Highlight box

Key findings

- Robotic-assisted computed tomography (CT)-guided interventional approach can effectively help inexperienced junior physicians to master the procedure and potentially to increase precision and reduce the complication.

What is known and what is new?

- The robotic-assisted approach allows to effectively execute the percutaneous insertion procedure in the CT-guided lung nodules localization and potentially reduce the complication.
- The robotic-assisted CT-guided percutaneous approach makes the interventional workflow easier and shortens the learning curve of the inexperienced junior physicians.

What is the implication, and what should change now?

- This study implies the robotic assistance can help the inexperienced junior physicians to simplify the procedure workflow, improve the CT-guided interventional ability, and has a broad application prospect.

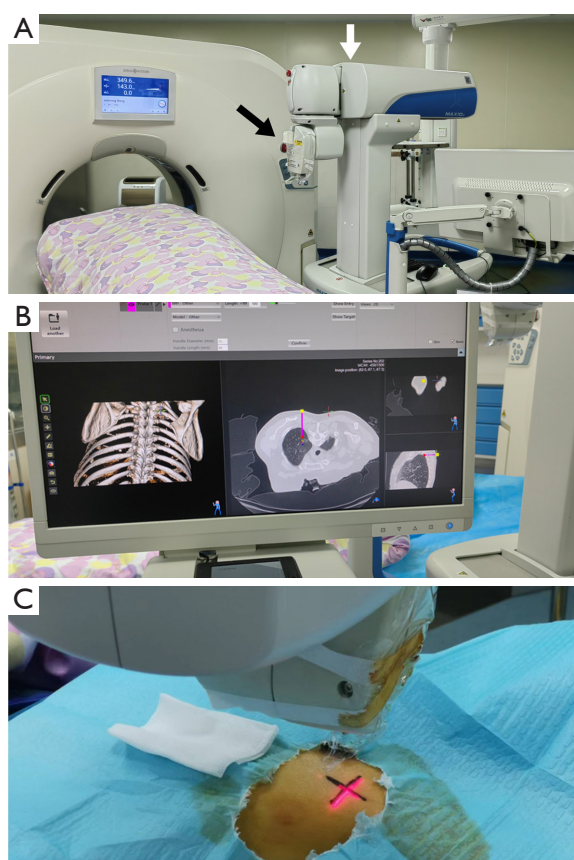


Figure 1 The robotic-assisted interventional radiological platform. (A) The robotic assistance platform (white arrow) is semi-automatically registered and docked at the CT table side, with the robotic arm (black arrow) positioned over the CT table. (B) The operator works out the puncture plan on the multiple plane reconstruction images and selects the appropriate needle length, depth and angulation using the interactive drop-down menus on the track pad. (C) Then the robotic arm automatically moves to the targeting area and the laser cross projects to the puncture point for the skin marker according to the previous plan. CT, computed tomography.

Robotic-assisted CT guidance

The robotic interventional radiologist assistance platform (MAXIO; Perfint Healthcare, Chennai, India) was semi-automatically registered and docked at the CT (Siemens, Somatom Definition Flash) tableside, with the robotic arm positioned over the CT table (*Figure 1A*). The patient firstly was immobilized well in a suitable position with vacuumed bean-bags. An initial plain scan CT (120 kV, 96 mAs, slice thickness 2 mm) was performed to identify

the nodule location and target region and images were manually transferred to the platform's workstation. The operator worked out the puncture plan on the multiple plane reconstruction images and selected the appropriate needle length, depth, and angulation using the interactive drop-down menus on the track pad (*Figure 1B*). Then the robotic arm automatically moved to the targeting area and the laser crosshair projected to the puncture entrance point as the skin marker according to the previous plan (*Figure 1C*).

Localization procedures

The pulmonary nodule localization device (Senscure, Ningbo, China) was used to perform preoperative target localization which consisted of the following five parts: coaxial needle (100 mm in length and 0.9 mm in diameter); pusher; anchor claw and suture; release buckle; protection tube (12). All CT-guided localizations were performed by two associate professors (H.Y. and Z.O.) in radiology who had been engaged in CT-guided intervention for less than 1 year but worked for more than 10 years as radiologists. After routine disinfection and local anesthesia, the needle was placed in the needle guide at the end effector of the arm. Then the operator inserted the needle through the skin marker and pushed the needle into the predetermined depth which normally should be within 10 mm around the pulmonary nodule avoiding into the nodule at the same slice on CT images. Once the needle was in place, the operator loosened the end effector and withdrew the robotic arm from the target area. A confirmatory CT plain scan of the targeting area was performed to automatically verify whether the actual puncture route was consistent with the plan and whether the needle placement was adequate on the platform's workstation. If the position of the needle did not meet the localization requirements, we manually made a small adjustment to the appropriate position without robotic assistance. The operator took the buckle off, pushed and released the anchor claw when the needle tip reached the proper target position. Then the operator pulled the pusher out of the coaxial needle completely and withdrew the needle tip to the outer rim of the pleura. Another CT plain scan of the target area was conducted to verify the withdrawal position of the needle before reinserting the pusher into the coaxial needle and pushing it to the end, resulting in the complete insertion of the suture into the pleural cavity. Subsequently, the needle and pusher were removed from the patient's body. The last CT plain scan was performed to determine the positional relation

between the nodules and the anchor claw and evaluate the complications such as pneumothorax, hemorrhage, etc. (Figure 2).

Conventional freehand group

In order to compare the effectiveness and safety of the robotic-assisted navigation system, the patients initially performed the conventional manual freehand CT-guided localization of SPNs from 19 August 2021 to 31 March 2022 by the same interventional radiologists team were selected as the control group.

Surgery

All patients accepted VATS under general anesthesia. During the operation, the nodule was easily and accurately located according to the direction of the suture by observing and pulling the suture with forceps, and wedge resection or segmentectomy of lung was performed surrounding the nodule. A lobectomy and systemic lymph node dissection were carried out if invasive adenocarcinoma was determined by the intra-operative frozen pathologic examination.

Data collection

Age, gender, nodule size, type, location, number, pathology, localization depth, localization time, complications, distance to pleura, and distance between anchor and lesion were manually recorded on the PACS workstation. Localization time was defined as the period from the first CT scan to the last CT scan. The time of VATS was calculated from inpatients' record, in addition, the operation time of 40 cases accepting VATS without preoperative location procedure was obtained as the control group. Unsuccessful localizations were evaluated, including dislodgement and exceeding the standard distance. Complications were evaluated including anchor claw dislodgement, pneumothorax, parenchymal hemorrhage, pleural reaction, and intercostal vascular hemorrhage on CT images.

Cumulative sum (CUSUM) analysis

In the present study, the CUSUM method was employed to evaluate the learning curve, measuring the accumulated variances between individual data points and the mean of all data points (16). The patients with single nodule were categorized in chronological order, and the localization

time, spent by two operators separately, was collected for calculating $CUSUM = \sum_{i=1}^n (x_i - \mu)$ (x_i and μ indicate individual localization time and the mean localization time, respectively).

Statistical analysis

The quantitative data were presented as mean and standard deviation for continuous variables, otherwise frequency and percentage were listed for categorical variables. Mann-Whitney U test was used for continuous variables, and χ^2 test was used for categorical variables. All statistical analyses were performed using Windows software SPSS (version 25; IBM, Armonk, NY, USA), and the significance level was set at 0.05.

Results

Characteristics of patient and lesion

Patient characteristics are shown in Table 1. A total of 599 patients (202 males and 397 females; average age, 53.84 ± 11.34 years; age range, 22–82 years) with 654 pulmonary nodules were eligible to enroll in this study. The nodules were classified as pure GGN [520 (79.51%)], mixed GGN [55 (8.41%)], solid [65 (9.94%)], and part cystic [14 (2.14%)]. The mean nodule size was 8.31 ± 3.59 mm, and the distance from nodules to the pleura was 12.32 ± 11.26 mm.

Localization procedure

All 654 nodules were marked using the new pulmonary nodule localization device. The time required for marking was 22.85 ± 10.27 min, and the average distance between the anchor and lesion was 5.01 ± 3.45 mm. The marking success rate was 96.64% (632/654). The localization failure of 22 nodules was due to dislodgement [2 (0.31%)] and the unsatisfactory position of the anchor [20 (3.06%)].

Overall, no deaths or other severe adverse events occurred during the study procedures. We found localization-related pneumothorax in 163 (27.21%) patients, including mild pneumothorax (the compressed lung <20%) in 156 (26.04%) patients and moderate or severe pneumothorax (the compressed lung >20%) in 7 (1.17%) patients. A total of 222 (33.94%) cases occurred parenchymal hemorrhage which did not require intervention, including mild hemorrhage [218 (33.33%)] and moderate hemorrhage [4 (0.61%)] occurred. The

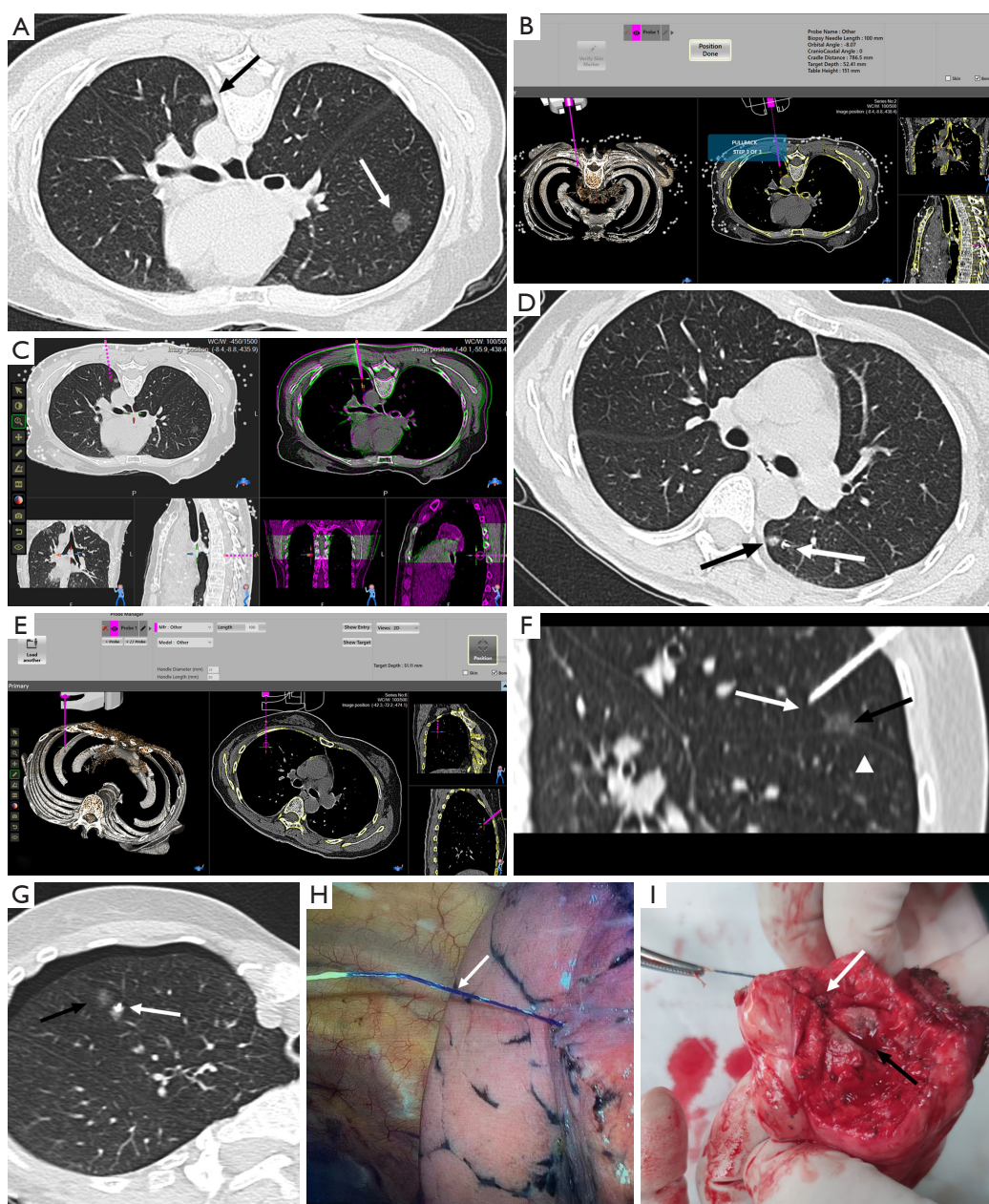


Figure 2 Example of two SPNs in the bilateral lungs undergoing robotic-assisted CT-guided localization. (A) A 10 mm pure GGN (white arrow) in the right upper lobe and a 6 mm mixed GGN (black arrow) in the left lower lobe need to be marked before VATS. (B) At first, the patient is placed in the prone position and the operator works out the puncture plan for the mixed GGN in the left lower lobe at the interface of the robotic assistant CT guidance system. (C) The image fusion of the planned scheme and the actual needle position shows only a small deviation. (D) Subsequently, post-localization CT shows the anchor (white arrow) is adjacent to the SPN (black arrow) and pneumothorax does not occur in the supine position. (E) The operator works out the out-of-plane puncture plan for the pure GGN in the right upper lobe at the interface. (F) Just like the planned scheme to avoid interlobar fissure (arrowhead), the needle tip (white arrow) is placed near the SPN (black arrow) and bypasses the interlobar fissure. (G) The last CT shows the anchor (white arrow) is adjacent to the SPN (black arrow) and mild pneumothorax and mild parenchymal hemorrhage occur. (H) During the VATS, the suture of needle (white arrow) accurately guides surgeon to locate the focus SPN. (I) The anchor claw (white arrow) and the marked SPN (black arrow) are displayed after VATS and its surrounding lung tissue. SPN, small pulmonary nodule; CT, computed tomography; GGN, ground-glass nodule; VATS, video-assisted thoracoscopic surgery.

Table 1 Characteristics of patients and nodules

Characteristics	Values
Number of patients	599
Age (years)	53.84±11.34
Gender	
Male	202 (33.72)
Female	397 (66.28)
Number of patients with marked nodules	
One nodule	548
Two nodules	47
Three nodules	4
Number of nodules	654
Size of nodules (mm)	8.31±3.59
Distance to pleura (mm)	12.32±11.26
Location of nodules (n=654)	
Right upper lobe	213 (32.57)
Right middle lobe	23 (3.52)
Right lower lobe	130 (19.88)
Left upper lobe	179 (27.37)
Left lower lobe	109 (16.67)
Type of nodule (n=654)	
Pure GGN	520 (79.51)
Mixed GGN	55 (8.41)
Solid	65 (9.94)
Part cystic	14 (2.14)

Values are shown as number, median ± standard deviation, or number (%). GGN, ground-glass nodule.

incidence of pleural reaction was 0.50% (3/599). And the rate of intercostal vascular hemorrhage was 0.83% (5/599) (*Table 2*).

Surgery and pathological results of targeted nodules

All targeted nodules were resected successfully and all devices were retrieved entirely during operation, which were then rapidly found and confirmed by pathologists. There were 316 nodules (48.32%) excised by wedge resection and 278 nodules (42.51%) resected with segmentectomy. Sixty lesions (9.17%) were later converted to lobectomy due to the determination of an invasive stage based on

Table 2 Characteristics of localization procedure

Characteristics	Values
Time of localization procedure (min)	22.85±10.27
Distance between anchor and lesion (mm) (n=654)	5.01±3.45
Successful localization	632 (96.64)
Unsuccessful localization	22 (3.36)
Dislodgement	2 (0.31)
Exceed the standard distance	20 (3.06)
Complications	
Pneumothorax (n=599)	163 (27.21)
Mild pneumothorax	156 (26.04)
Moderate or severe pneumothorax	7 (1.17)
Parenchymal hemorrhage (n=654)	222 (33.94)
Mild hemorrhage	218 (33.33)
Moderate hemorrhage	4 (0.61)
Pleural reaction (n=599)	3 (0.50)
Intercostal vascular hemorrhage (n=599)	5 (0.83)

Values are shown as mean ± standard deviation or number (%).

the intraoperative frozen section analysis with the specific micropapillary and solid histological patterns. The time of VATS was 95.21±47.28 min. Histopathological examination revealed 166 (25.38%) benign nodules and 488 (74.62%) malignant nodules (*Table 3*).

Learning curve analysis

In this study, we included 251 (by operator 1) and 297 (by operator 2) patients, respectively. We utilized the CUSUM method to analyze the chronological localization time and constructed the learning curve, depicted in *Figure 3*. This visualization illustrates the evolution of operation time with increasing experience. Notably, two pivotal points emerged at the 50th and 90th cases, leading to the division of the learning curve into three distinct phases:

- ❖ Phase I (initial 50 cases): during this phase, the localization time exceeded the average, and the learning curve exhibited a steep upward trend, indicating a rapid growth in operation time.
- ❖ Phase II (50th to the 90th case): in this phase, the localization time continued to surpass the average, albeit with a gradually ascending trend in the learning curve. This suggests a slower rate of

Table 3 Surgical characteristics and pathological results of localized nodules

Characteristics	Values
Retrieving of device after resection	654 (100.00)
Time of VATS (min)	95.21±47.28
Resection	
Wedge resection	316 (48.32)
Segmentectomy	278 (42.51)
Lobectomy	60 (9.17)
Postoperative pathological results	
Invasive adenocarcinoma	94 (14.37)
Minimally invasive adenocarcinoma	180 (27.52)
Adenocarcinoma <i>in situ</i>	212 (32.42)
Benign lesion	166 (25.38)
Other malignant tumors	2 (0.31)

Values are shown as number (%) or mean ± standard deviation.
VATS, video-assisted thoracoscopic surgery.

improvement compared to the initial phase.

- ❖ Phase III (after the 90th case): subsequent to the 90th case, the localization time fell below the average, and the curve displayed a consistent downward trend.

The changes in operation time after localization

To more accurately display the changes in operation time after localization, we selected Dr. Du (with more than 10 years of clinical experience in single-port VATS), who had the most operations in our study and removed all nodules with single-port VATS after localization. The time of wedge resections and segmentectomies was calculated, excluding multiple nodules, and 55 wedge resections and 18 segmentectomies were incorporated into the study. We randomly picked 40 single-port VATS (from January 2019 to December 2020) with routine HRCT/three-dimensional (3D) by Dr. Du as the control group, including 20 wedge resections and 20 segmentectomies. For patients who

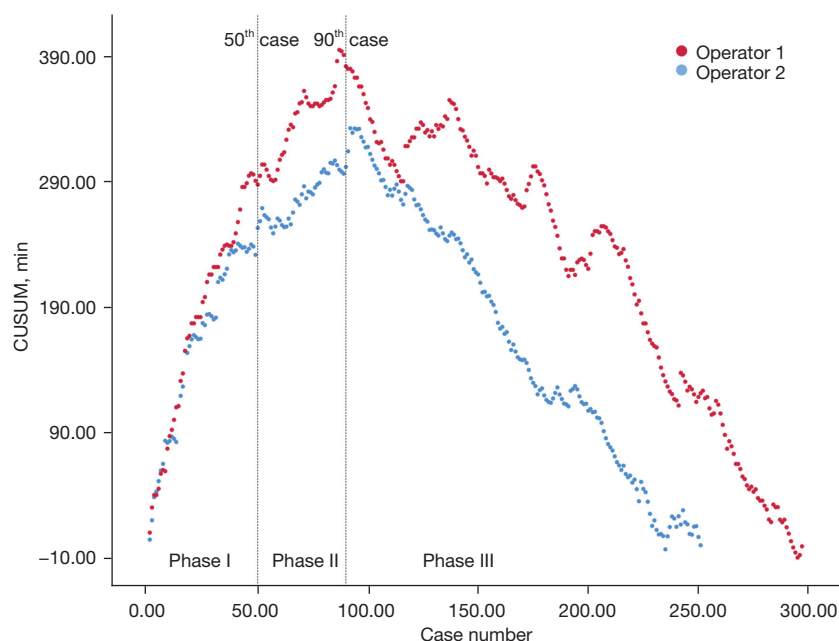


Figure 3 The CUSUM curve of localization time. As shown in the curve, two cutoff points are found in the 50th case and the 90th case. The learning curve is divided into three phases: phase I (the initial 50 cases), phase II (the 50th to the 90th case), and phase III (after the 90th case). CUSUM, cumulative sum.

Table 4 Comparison of surgical time

Surgical method	After only routine HRCT/3D	After localization with needle	Shorten time (%)	P value
Wedge resection (min)	66.80±21.30 (n=20)	56.27±16.39 (n=55)	15.76	0.04
Segmentectomy (min)	167.50±40.70 (n=20)	93.61±35.72 (n=18)	44.11	<0.001

Values are shown as mean ± standard deviation (number). HRCT, high resolution computed tomography; 3D, three-dimensional.

Table 5 Comparison of safety and efficiency

Efficiency and complications	Robotic-assisted group	Conventional manual group	P value
Time of localization procedure (min)	22.85±10.27 (n=599)	21.88±8.40 (n=90)	0.48
Distance between anchor and lesion (mm)	5.01±3.45 (n=654)	4.60±3.46 (n=94)	0.71
Complications			
Pneumothorax	163/599 (27.21)	39/90 (43.33)	0.002
Parenchymal hemorrhage	222/654 (33.94)	26/94 (27.66)	0.23

Values are shown as mean ± standard deviation (number) or number/total (%).

received localizations, the time of VATS was significantly shorter, especially for the segmentectomy group (93.61±35.72 *vs.* 167.50±40.70 min, *P*<0.001) (Table 4).

Comparisons with conventional manual CT-guided localization

A total of 90 patients (37 males and 53 females) with 94 SPNs (four patients with two SPNs) were selected to as the control group. There were significant differences in the time of localization procedure (*P*=0.48), the distance between anchor and lesion (*P*=0.71), and parenchymal hemorrhage (*P*=0.23) between the robotic-assisted group and the conventional manual group. However, compared with the traditional manual group, the proportion of pneumothorax in the robotic-assisted group significantly decreased (27.21% *vs.* 43.33%, *P*=0.002) (Table 5).

Discussion

In this study, we applied a robotic-assisted navigation technology to CT-guided SPNs localization marked by a hook-wire needle and demonstrated that it was a safe, feasible, and effective procedure for leading VATS to remove pulmonary nodules.

Studies have revealed that the robotic-guided approach appears to be safe, with high accuracy and a comparable radiation dose to patients for CT-guided interventional operation (8,9,17-21). In our study, both operators were

less experienced beginners in CT intervention, and we conducted the procedure of targeting preoperative SPNs combining the modified localization device under the robotic navigated CT guidance for rapidly improving the CT interventional capability. After proficiently mastering the robotic system operation, patients usually only required one puncture and three CT scans for most of the localization procedure of pulmonary nodules. In particular, robotic navigation was very valuable for complex procedures of CT-guided pulmonary nodule localization demanding needle insertion with multiple planes and angulations (such as out-of-plane path) (Figure 3).

In this study, the time of localization (22.85±10.27 min) was longer than the previous operating time (14.4±6.6 min) reported by Fan *et al.* (22). First, 51 patients (8.51%) with multiple nodules were included in our study, and localization of multiple nodules certainly resulted in a significant increase in operating time. Secondly, this difference might be related to the application of the sterile cover and to some technical issues with data transfer and device control, which is similar to the study reported by Heerink *et al.* (20). In addition, due to the less experienced beginners of our operators, we stipulated that most patients needed to undergo the delayed CT scan to detect the progressive complications after 5 min of finishing localization in the initial stage on the learning curve. The mean localization time had dropped to 18.86±5.49 min in phase III based on the learning curve.

Robotic-assisted CT-guided percutaneous pulmonary

nodule localization maintained a high marking success rate (96.64%) in this study, which was higher than that of localization with hook-wire or microcoil (22,23), even if our operators were less experienced. The robotic navigated system provides a simple human-machine interaction operation for operators to choose appropriate puncture points, angles, and depths, making the puncture plan and performance easier for radiologists with insufficient interventional experience. To avoid the impact of patient's breath depth and result in deviations between the pre-planned plane and the insertion position, each operating doctor reminded patients to free breathe calmly and avoid deep breathing and coughing before location. In addition, we applied a vacuum negative pressure pad to assist patients in maintaining a relatively comfortable fixed position. Most of the unsuccessful localizations were due to the marking distance between the anchor and nodules being more than 10 mm, however, these localizations also successfully guided surgeons to locate and resect the nodules. Besides, marking failure included anchor of dislodgement in 2 cases (0.31%) which occurred in the very early attempts. After carefully analyzing the reasons, the dislodgement of two cases was not caused by the robotic-assisted platform or localization device, but was due to the location of nodules (below the pleura) and the fact that the locating needle tip was too shallow. Puncturing out of pleura led to dislodgement owing to lung collapse. Thus, for patients with subpleural nodules, it is suggested that the tip of the needle is punctured over 1cm deep in the pleura or placed in the deeper area than the nodule to reduce the probability of unhooking.

It is commonly known that inexperienced physicians with the new device might increase the complication rate (22), but the safety and complication incidence of our robotic-assisted approach were satisfactory in this study. No cases with severe fatal complications such as air embolism and cerebral or myocardial infarction occurred in our cohort. Localization-related pneumothorax occurred in 163 (27.21%) patients however, most of them belonged to mild pneumothorax that did not require special treatment. Only 7 (1.17%) patients experienced moderate or severe pneumothorax and then they were transferred to operating room for surgery soon. In addition, 33.94% of cases (222/654) experienced parenchymal hemorrhage. The incidence of pneumothorax and hemorrhage was similar to a previous study by Huang *et al.* (24), but higher than localization with the same needle reported (12,22,23). In our study, even very little pneumothorax and hemorrhage were also counted into the complications which might

result in the relatively high incidence rate. Intercoastal vascular hemorrhage and pleural reaction are not reported in previous studies with the modified hook-wire localization needle. The rate of pleural reaction was 0.50% (3/599) in our study, which is lower than previous studies using hook wire needles without improvement (22,25), and all patients gained relief spontaneously by symptomatic treatment. All five cases of intercoastal vascular hemorrhage were due to inappropriate paths with lack of experience or variant artery route, then they were immediately transferred into the operation room and got the surgical treatment.

Few studies investigated the learning process of CT-guided interventional radiology under robotic assistance. According to the learning curve for percutaneous transthoracic needle biopsy of thoracic imaging, about 90–100 procedures are required to achieve acceptable diagnostic performance and obtain an acceptable false-negative rate (26,27). In our study, our two operators almost simultaneously reached phase I and II in the 50th and 90th case, although variability of learning speed among operators had been reported in different medical skills (28). All our team members (operators, nurses, and technologists) lacked of relevant experience in the early stage and cautiously learned the methods of preoperative SPNs localization under the robotic-guided system. That was why most patients needed a substantial amount of time for localization in phase I. In phase II, the learning curve displayed a slow growth trend through continuously improving the workflow and gradually practicing difficult operations, such as localization for multiple SPNs and pulmonary nodules near the great vessels or heart, or covered by the scapula. Our operators have already mastered the processing techniques so sensibly shortened the localization duration by strengthening training and summarizing the experience in phase III. We trusted the learning curve displayed in our study would help to accurately understand the benefit of using the robotic-assisted navigation system in CT-guided interventional procedures for less experienced physicians.

We found that this preoperative localization approach of pulmonary nodules can significantly shorten the surgical time. The effectiveness of robotic-assisted CT-guided preoperative localization was confirmed by our results (after localization with needles, the wedge resection group and segmentectomy decreased by 15.76% and 44.11% respectively compared to conventional methods) for VATS. It was undeniable that due to the assistance of our preoperative localization, the surgeons dared to perform more difficult VATS such as the pure GGNs and deep

small nodules which might be too tiny in density or size to palpate. In wedge resection, the pathological examination took up a large proportion of time during the whole operation. So that this localization also obviously reduced the time of detecting the responsible nodule by pathologists.

Compared to the patients who underwent conventional manual CT-guided localization of SPNs, the incidence of pneumothorax in the robotic-assisted localization group showed a significant decrease [27.21% (163/599) *vs.* 43.33% (39/90)], which could be attributed to less frequency and time of adjustments with robotic assistance. Furthermore, the proportion of multiple nodules localization in the robotic-assisted localization group was also more than in the conventional manual localization group [8.51% (51/599) *vs.* 4.44% (4/90)]. While, the time of localization procedure, distance between anchor and lesion, and parenchymal hemorrhage were similar in the two groups. These indicated that robot-assisted technique might potentially increase the precision and reduce the complication. To our knowledge, in addition to our research, there are only a small number of studies on small samples of humans or animals about robotic-assisted CT-guided localization of SPNs (29–31). In the future, we will design prospective cohort studies to further compare two technical methods.

There are limitations in this study. First, the study was a single-center retrospective study, rather than a randomized controlled prospective study. Second, this study did not assess pain during the localization. At last, this study focused primarily on inexperienced radiologists rather than sophisticated doctors.

Conclusions

Robotic-assisted CT-guided percutaneous pulmonary nodules hook-wire localization could be effectively helpful for junior less experienced interventional physicians to master the procedure and potentially increase precision. In other words, robot techniques would be able to provide beginners more accurate and safe technology for interventional procedures.

Acknowledgments

Funding: None.

Footnote

Reporting Checklist: The authors have completed the

STROBE reporting checklist. Available at <https://jtd.amegroups.com/article/view/10.21037/jtd-24-198/rc>

Data Sharing Statement: Available at <https://jtd.amegroups.com/article/view/10.21037/jtd-24-198/dss>

Peer Review File: Available at <https://jtd.amegroups.com/article/view/10.21037/jtd-24-198/prf>

Conflicts of Interest: All authors have completed the ICMJE uniform disclosure form (available at <https://jtd.amegroups.com/article/view/10.21037/jtd-24-198/coif>). The authors have no conflicts of interest to declare.

Ethical Statement: The authors are accountable for all aspects of the work in ensuring that questions related to the accuracy or integrity of any part of the work are appropriately investigated and resolved. The study was conducted in accordance with the Declaration of Helsinki (as revised in 2013). This retrospective study was approved by the Ethics Committee of the First Affiliated Hospital of Chongqing Medical University (No. ES-2023-020-01). The requirement for informed consent was waived for this retrospective analysis.

Open Access Statement: This is an Open Access article distributed in accordance with the Creative Commons Attribution-NonCommercial-NoDerivs 4.0 International License (CC BY-NC-ND 4.0), which permits the non-commercial replication and distribution of the article with the strict proviso that no changes or edits are made and the original work is properly cited (including links to both the formal publication through the relevant DOI and the license). See: <https://creativecommons.org/licenses/by-nc-nd/4.0/>.

References

1. de Koning HJ, van der Aalst CM, de Jong PA, et al. Reduced Lung-Cancer Mortality with Volume CT Screening in a Randomized Trial. *N Engl J Med* 2020;382:503–13.
2. Tsutani Y, Handa Y, Shimada Y, et al. Comparison of cancer control between segmentectomy and wedge resection in patients with clinical stage IA non-small cell lung cancer. *J Thorac Cardiovasc Surg* 2021;162:1244–1252.e1.
3. Chao YK, Pan KT, Wen CT, et al. A comparison of efficacy and safety of preoperative versus intraoperative computed

- tomography-guided thoroscopic lung resection. *J Thorac Cardiovasc Surg* 2018;156:1974-1983.e1.
4. Lin FC, Tsai SC, Tu HT, et al. Computed tomography-guided localization with laser angle guide for thoracic procedures. *J Thorac Dis* 2018;10:3824-8.
 5. Chen A, Pastis N, Furukawa B, et al. The effect of respiratory motion on pulmonary nodule location during electromagnetic navigation bronchoscopy. *Chest* 2015;147:1275-81.
 6. Kondo R, Yoshida K, Hamanaka K, et al. Intraoperative ultrasonographic localization of pulmonary ground-glass opacities. *J Thorac Cardiovasc Surg* 2009;138:837-42.
 7. Beyer LP, Pregler B, Michalik K, et al. Evaluation of a robotic system for irreversible electroporation (IRE) of malignant liver tumors: initial results. *Int J Comput Assist Radiol Surg* 2017;12:803-9.
 8. Mbalisike EC, Vogl TJ, Zangos S, et al. Image-guided microwave thermoablation of hepatic tumours using novel robotic guidance: an early experience. *Eur Radiol* 2015;25:454-62.
 9. Schaible J, Pregler B, Verloh N, et al. Improvement of the primary efficacy of microwave ablation of malignant liver tumors by using a robotic navigation system. *Radiol Oncol* 2020;54:295-300.
 10. Sato M. Precise sublobar lung resection for small pulmonary nodules: localization and beyond. *Gen Thorac Cardiovasc Surg* 2020;68:684-91.
 11. Fan L, Yang H, Yu L, et al. Multicenter, prospective, observational study of a novel technique for preoperative pulmonary nodule localization. *J Thorac Cardiovasc Surg* 2020;160:532-539.e2.
 12. Li CD, Huang ZG, Sun HL, et al. Marking ground glass nodules with pulmonary nodules localization needle prior to video-assisted thoracoscopic surgery. *Eur Radiol* 2022;32:4699-706.
 13. Qin W, Ge J, Gong Z, et al. The incidence and risk factors of acute pain after preoperative needle localization of pulmonary nodules: a cross-sectional study. *Transl Lung Cancer Res* 2022;11:1667-77.
 14. Jin X, Wang T, Chen L, et al. Single-Stage Pulmonary Resection via a Combination of Single Hookwire Localization and Video-Assisted Thoracoscopic Surgery for Synchronous Multiple Pulmonary Nodules. *Technol Cancer Res Treat* 2021;20:15330338211042511.
 15. Wu X, Li T, Zhang C, et al. Comparison of Perioperative Outcomes Between Precise and Routine Segmentectomy for Patients With Early-Stage Lung Cancer Presenting as Ground-Glass Opacities: A Propensity Score-Matched Study. *Front Oncol* 2021;11:661821.
 16. Yu J, Rao S, Lin Z, et al. The learning curve of endoscopic thyroid surgery for papillary thyroid microcarcinoma: CUSUM analysis of a single surgeon's experience. *Surg Endosc* 2019;33:1284-9.
 17. Beyer LP, Pregler B, Niessen C, et al. Robot-assisted microwave thermoablation of liver tumors: a single-center experience. *Int J Comput Assist Radiol Surg* 2016;11:253-9.
 18. de Baère T, Roux C, Deschamps F, et al. Evaluation of a New CT-Guided Robotic System for Percutaneous Needle Insertion for Thermal Ablation of Liver Tumors: A Prospective Pilot Study. *Cardiovasc Intervent Radiol* 2022;45:1701-9.
 19. Tinguely P, Paolucci I, Ruiter SJS, et al. Stereotactic and Robotic Minimally Invasive Thermal Ablation of Malignant Liver Tumors: A Systematic Review and Meta-Analysis. *Front Oncol* 2021;11:713685.
 20. Heerink WJ, Ruiter SJS, Pennings JP, et al. Robotic versus Freehand Needle Positioning in CT-guided Ablation of Liver Tumors: A Randomized Controlled Trial. *Radiology* 2019;290:826-32.
 21. Abdullah BJ, Yeong CH, Goh KL, et al. Robotic-assisted thermal ablation of liver tumours. *Eur Radiol* 2015;25:246-57.
 22. Fan L, Ma W, Ma J, et al. The improved success rate and reduced complications of a novel localization device vs. hookwire for thoracoscopic resection of small pulmonary nodules: a single-center, open-label, randomized clinical trial. *Transl Lung Cancer Res* 2022;11:1702-12.
 23. Li CD, Huang ZG, Sun HL, et al. CT-guided preoperative localization of ground glass nodule: comparison between the application of embolization microcoil and the locating needle designed for pulmonary nodules. *Br J Radiol* 2021;94:20210193.
 24. Huang YY, Wang T, Fu YF, et al. Comparison of the effectiveness of anchoring needles and coils in localizing multiple nodules in the lung. *BMC Pulm Med* 2022;22:393.
 25. Seo JM, Lee HY, Kim HK, et al. Factors determining successful computed tomography-guided localization of lung nodules. *J Thorac Cardiovasc Surg* 2012;143:809-14.
 26. Ahn SY, Park CM, Yoon SH, et al. Learning Curve of C-Arm Cone-beam Computed Tomography Virtual Navigation-Guided Percutaneous Transthoracic Needle Biopsy. *Korean J Radiol* 2019;20:844-53.
 27. Fontaine-Delaruelle C, Souquet PJ, Gamondes D, et al. Negative Predictive Value of Transthoracic Core-Needle Biopsy: A Multicenter Study. *Chest* 2015;148:472-80.

28. Kemp SV, El Batrawy SH, Harrison RN, et al. Learning curves for endobronchial ultrasound using cusum analysis. *Thorax* 2010;65:534-8.
29. Zhou G, Chen X, Niu B, et al. Intraoperative localization of small pulmonary nodules to assist surgical resection: A novel approach using a surgical navigation puncture robot system. *Thorac Cancer* 2020;11:72-81.
30. Liu J, Jiang Y, He R, et al. Robotic-assisted navigation system for preoperative lung nodule localization: a pilot study. *Transl Lung Cancer Res* 2023;12:2283-93.
31. Duan X, He R, Jiang Y, et al. Robot-assisted navigation for percutaneous localization of peripheral pulmonary nodule: an in vivo swine study. *Quant Imaging Med Surg* 2023;13:8020-30.

Cite this article as: Guo H, Ouyang Z, Li X, Han Y, Tao F, Liu M, Cheng R, Chen X, Lv F, Yang H. Robotic-assisted CT-guided percutaneous pulmonary nodules localization by hook-wire needles: a retrospective observational study. *J Thorac Dis* 2024;16(7):4263-4274. doi: 10.21037/jtd-24-198